

Journal of General Virology

High Throughput Screening of a GlaxoSmithKline Protein Kinase Inhibitor Set Identifies an Inhibitor of Human Cytomegalovirus Replication that Prevents CREB and Histone H3 Post-Translational Modification

--Manuscript Draft--

Manuscript Number:	JGV-D-16-00474R3
Full Title:	High Throughput Screening of a GlaxoSmithKline Protein Kinase Inhibitor Set Identifies an Inhibitor of Human Cytomegalovirus Replication that Prevents CREB and Histone H3 Post-Translational Modification
Article Type:	Standard
Section/Category:	Animal - Large DNA Viruses
Corresponding Author:	Blair L Strang St George's Medical School UNITED KINGDOM
First Author:	Amina S Khan
Order of Authors:	Amina S Khan Matthew J Murray Catherine M K Ho William J Zuercher Matthew B Reeves Blair L Strang
Abstract:	<p>To identify new compounds with anti-human cytomegalovirus (HCMV) activity and new anti-HCMV targets, we developed a high throughput strategy to screen a GlaxoSmithKline (GSK) Published Kinase Inhibitor Set (PKIS). This collection contains a range of extensively characterized compounds grouped into chemical families (chemotypes). From our screen we identified compounds within chemotypes that impede HCMV replication and identified kinase proteins associated with inhibition of HCMV replication that are potential novel anti-HCMV targets. We focused our study on a top "hit" in our screen, SB-734117, which we found inhibits productive replication of several HCMV strains. Kinase selectivity data indicated that SB-734117 exhibits polypharmacology and is an inhibitor of several proteins from the AGC and CMCG kinase groups. Using western blotting we found that SB-734711 inhibited accumulation of HCMV immediate-early proteins, phosphorylation of cellular proteins involved in immediate-early protein production (CREB and histone H3) and histone H3 lysine 36 trimethylation (H3K36me3). Therefore, we identify SB-734117 as a novel anti-HCMV compound and find that inhibition of AGC and CMCG kinase proteins during productive HCMV replication is associated with inhibition of viral protein production and prevents post-translational modification of cellular factors associated with viral protein production.</p>



Click here to access/download
Response to Reviewer
Response.docx



1
2
3
4
5
6
7
8
9
10
11
12
13
14
15
16
17
18
19
20
21
22
23

STANDARD RESEARCH ARTICLE

High Throughput Screening of a GlaxoSmithKline Protein Kinase Inhibitor Set
Identifies an Inhibitor of Human Cytomegalovirus Replication that Prevents
CREB and Histone H3 Post-Translational Modification

Amina S Khan¹, Matthew J Murray², Catherine M K Ho¹, William J Zuercher³
Matthew B Reeves² & Blair L Strang^{1,4}

Institute of Infection & Immunity, St George's, University of London, London, UK¹;
Institute of Immunity & Transplantation, University College London, London, UK²;
Eshelman School of Pharmacy, University of North Carolina, Chapel Hill, NC,
USA³; Department of Biological Chemistry & Molecular Pharmacology, Harvard
Medical School, Boston, MA, USA⁴

A.S.K. and B.L.S. contributed equally to this work.

Running Title: Screening Kinase Inhibitors Targeting HCMV

Corresponding Author: BLS (bstrang@sgul.ac.uk, +44 (0)208 725 3866)

Keywords: human cytomegalovirus, screening, kinase, CREB, histone

Subject Category: Animal - DNA Viruses

Word Count (Abstract and Main Text): 6,630 (193 and 6,437)

24 **ABSTRACT**

25

26 To identify new compounds with anti-human cytomegalovirus (HCMV)
27 activity and new anti-HCMV targets, we developed a high throughput strategy to
28 screen a GlaxoSmithKline (GSK) Published Kinase Inhibitor Set (PKIS). This
29 collection contains a range of extensively characterized compounds grouped into
30 chemical families (chemotypes). From our screen we identified compounds within
31 chemotypes that impede HCMV protein production and identified kinase proteins
32 associated with inhibition of HCMV protein production that are potential novel
33 anti-HCMV targets. We focused our study on a top “hit” in our screen, SB-
34 734117, which we found inhibits productive replication of several HCMV strains.
35 Kinase selectivity data indicated that SB-734117 exhibits polypharmacology and
36 is an inhibitor of several proteins from the AGC and CMCG kinase groups. Using
37 western blotting we found that SB-734711 inhibited accumulation of HCMV
38 immediate-early proteins, phosphorylation of cellular proteins involved in
39 immediate-early protein production (CREB and histone H3) and histone H3 lysine
40 36 trimethylation (H3K36me3). Therefore, we identify SB-734117 as a novel
41 anti-HCMV compound and find that inhibition of AGC and CMCG kinase proteins
42 during productive HCMV replication is associated with inhibition of viral protein
43 production and prevents post-translational modification of cellular factors
44 associated with viral protein production.

45 **INTRODUCTION**

46

47 Disease associated with human cytomegalovirus (HCMV) infection affects
48 a range of immunodeficient individuals [1]. As yet, there is no widely available
49 vaccine against HCMV [2] and disease management largely rests on the use of
50 anti-HCMV drugs [1, 3]. The most widely used anti-HCMV drugs (including the
51 frontline drug ganciclovir) target the viral DNA polymerase, thereby inhibiting
52 HCMV replication [3]. However, there are drawbacks to the use of ganciclovir
53 and other currently available anti-HCMV drugs, including the development of
54 drug resistant virus [3]. Furthermore, HCMV not only undergoes productive
55 replication but can also enter a latent state from which the virus can reactivate.
56 Currently, there is no effective treatment to clear latent HCMV infection.

57 Several novel anti-HCMV drugs are under development [1, 3, 4]. One
58 strategy to expand the range of anti-HCMV drugs available is to identify existing
59 compounds with hitherto unappreciated anti-HCMV activity. A large number of
60 currently available compounds inhibit protein kinases in each of the groups that
61 comprise the human kinome. Protein kinases are involved in many aspects of
62 HCMV replication and pathogenesis, including intracellular signaling that results
63 in transcription from the HCMV major immediate early promoter (MIEP), which
64 stimulates a transcriptional cascade (*immediate-early* to *early* to *late* gene
65 transcription) required for productive HCMV replication and reactivation from
66 latency [1]. Therefore, protein kinase inhibitors could inhibit productive HCMV
67 replication or reactivation from latency and a number of kinase inhibitors with

68 anti-HCMV activity have been identified [3]. Furthermore, it is possible that the
69 full complement of protein kinases that are required for HCMV replication have
70 yet to be identified. Therefore, kinase inhibitors could be used as chemical
71 probes to identify kinase proteins required for HCMV replication, many of which
72 could be novel anti-HCMV drug targets. However, an important consideration
73 when using kinase inhibitors is that compounds targeting the conserved ATP-
74 binding site of a kinase protein can display polypharmacology and are capable of
75 inhibiting several kinase proteins or proteins outside the kinome, such as G-
76 protein coupled receptors (GPCRs) [5-7]. Therefore, knowledge of kinase
77 selectivity is important when discussing the use of kinase inhibitors as drugs or
78 chemical probes [5].

79 We utilized a high throughput screening methodology to assess the ability
80 of compounds within a GlaxoSmithKline (GSK) Published Kinase Inhibitor Set
81 (PKIS) [8] to inhibit HCMV protein production. This compound library contained a
82 range of extensively characterized compounds organized into structurally related
83 collections of compound families (chemotypes) [7, 8]. Known characteristics of
84 compounds within this GSK PKIS collection include kinase selectivity, compound
85 structures and off-targets effects. Therefore, screening of this compound library
86 allowed identification of both compounds and chemotypes with anti-HCMV
87 activity, identification of novel anti-HCMV drug targets and permitted the on and
88 off-targets effects of compounds identified in the screening process to be
89 considered. These data lead to investigation of the anti-HCMV activity of a top
90 “hit” in our screen, SB-734117.

91 **RESULTS**

92

93 **High throughput screening of a GSK PKIS library to identify protein**
94 **kinase inhibitors with anti-HCMV activity.** To identify compounds with anti-
95 HCMV activity we utilized a high throughput screening methodology (Fig. 1(a)),
96 similar to the approach that we have previously used to screen siRNAs in HCMV
97 infected cells [9]. Briefly, high passage HCMV strain AD169 and compounds from
98 the GSK PIKS collection (listed in Table S1) were added to duplicate 384-well
99 plates seeded with human foreskin fibroblast (HFF) cells. As negative and
100 positive controls for compound treatment several wells in each plate were treated
101 with either DMSO or heparan sulphate (a small molecule that inhibits HCMV
102 entry into cells [10]), respectively. At 72 hours post infection (h.p.i.) cells were
103 stained with Hoescht 33342 to detect nuclear DNA and CellMask to detect the
104 area of the cell, plus were treated with antibodies to detect the cytoplasmic
105 HCMV antigen pp28. An automated microscopy system was then used to assay
106 both the number of cells in each well and the number of infected cells in each
107 well expressing pp28. An image of infected cells treated as described above and
108 captured using automated microscopy is shown in Fig. 1(b).

109 The mean number of cells in each well per plate was determined. Where
110 the number of cells in any well was less than 2-fold below the mean number of
111 cells of the plate, the compound in that well was judged to be cytotoxic (listed by
112 chemotype in Table 1 and by compound in Table S2). Data from the remaining
113 wells on duplicate plates were combined and converted to a z-score (the number

114 of standard deviations from the mean of the data [11, 12]) to demonstrate the
115 increase (positive z-score) or decrease (negative z-score) in the number of pp28
116 positive cells in presence of each compound (shown in Fig. 1(c), listed by
117 chemotype in Table 1 and by compound in Table S3).

118

119 **Analysis of cytotoxic compounds.** We first investigated what
120 compounds within chemotypes were judged to be cytotoxic. Approximately 40-
121 50% of compounds in the benzimidazole N-thiophene, 2H-3 pyrimidinyl
122 pyrazolopyridazine, 3-amino pyrazolopyridines and 6-phenyl isoquinolines
123 chemotypes contained compounds judged to be cytotoxic to HCMV infected cells
124 (Table 1 and Table S2). Therefore, compounds from these chemotypes are
125 generally not suitable for further use.

126 We then utilized kinase selectivity data to investigate which kinase
127 proteins were inhibited by each compound judged to be cytotoxic (Table S4).
128 Kinase selectivity data [7] lists the ability of each compound to inhibit a panel of
129 224 kinase proteins from several protein groups of the human kinome (including
130 TK, STE, AGC, S-T-PK, CAMK and CMCG groups). We found that all cytotoxic
131 benzimidazole N-thiophenes were potent inhibitors of PLK-1, whose inhibition
132 can lead to apoptosis, and nearly all other cytotoxic compounds from a number
133 of chemotypes were potent inhibitors of a range of CDK proteins, which are
134 involved in regulation of the cell cycle. In our screen cytotoxicity was judged by
135 the number of cells detected in each well of the screening plate. Therefore, we
136 concluded that compounds were generally judged to be cytotoxic due to

137 apoptosis associated with inhibition of PLK-1 or due to lack of cell division
138 associated with inhibition of CDK function.

139

140 **Analysis of compounds assigned z-scores.** Next, we analyzed those
141 compounds assigned z-scores to determine which compounds and chemotypes
142 should be considered for further study as anti-HCMV compounds and chemical
143 probes. We found that nearly all chemotypes contained compounds that had both
144 positive and negative effects on pp28 production. Notably, however, the 2-aryl 3-
145 pyridimidinyl pyrazolopyridazine and furopyrimidine chemotypes and the 3-vinyl
146 pyridine, 2,4-diamino pyrimidine, maleimide, phenyl carboxamide and indazole-5-
147 carboxamide chemotypes contained a large number of compounds with negative
148 and positive effects on pp28 production, respectively (Tables 1 and S3). We
149 sought to further characterize the results of our screen and judged any
150 compound with a z-score between 1 to -1 to have little or no effect on pp28
151 production, whereas compounds with z-scores of -1 to -2 and 1 to 2 had modest
152 negative or positive effects on pp28 production, respectively. Thusly, compounds
153 with z-scores of less than -2 or more than 2 had the greatest negative or positive
154 effect on pp28 production, respectively. Therefore, three compounds
155 (GW575808A, GW874091X and GW627512B) from three different chemotypes
156 (2,4-diamino pyrimidines, imidazotriazines, 2-amino oxazoles, respectively) had
157 strong positive effects on pp28 production, while four compounds (GW297361X,
158 SB-734117, SB-220025-R and GW795493X) from four chemotypes (oxindoles,
159 furazan benzimidazoles, 4-pyrimidinyl ortho-aryl azoles, furopyrimidines,

160 respectively) had strong negative effects on pp28 production (Figs. 1(c) and
161 1(d)).

162

163 **Examination of kinase protein inhibition by compounds assigned z-**
164 **scores.** We then examined kinase selectivity data of compounds assigned z-
165 scores (Table S5). The data from Table S5 is presented in Figure 2 as a
166 “heatmap” of kinase inhibition. Nearly all compounds assigned z-scores exhibited
167 polypharmacology and could inhibit more than one kinase protein. Consistent
168 with our analysis of compounds judged to be cytotoxic (Table S2), we found that
169 less than 5% of all compounds either potently inhibited PLK-1 or were potent
170 inhibitors of several different CDK proteins (Table S5). Compounds with positive
171 or negative z-scores were inhibitors of a wide range of kinase proteins in the TK
172 kinase group (Fig. 2 and Table S5). Therefore, inhibition of TK kinases alone was
173 unlikely to positively or negatively influence pp28 production. However, a number
174 of kinases in the STE (including MAP4K4 and MNK), CAMK (including PRKD1,
175 PRKD2 and PRKD3) and CMCG (including CLK2, HIPK1, HIPK4, DYRK1A,
176 DYRK1B, DYRK2) kinase groups were inhibited by compounds assigned z-
177 scores of less than -1 from 8, 4 and 3 different chemotypes, respectively (Figs.
178 2(a)-(c), respectively, and Table S5). Therefore, these kinase proteins, alone or
179 in combination, were likely to be important for HCMV replication and could
180 represent future anti-HCMV drug targets. A number of compounds from two
181 different chemotypes that inhibited kinases in AGC kinase family (including
182 PRKG1, PRKG2, PRKX, PKA, ROCK1, ROCK2) were assigned z-scores over 1

183 (Fig. 2(d)). Therefore, these kinase proteins, alone or in combination, were likely
184 to be inhibitory to HCMV replication. Compounds targeting these kinase proteins
185 are likely to be of little value as anti-HCMV drugs.

186 Compounds assigned z-scores of less than -2 (GW297361X, SB-734117,
187 SB-220025-R and GW795493X) each had a distinct kinase selectivity profile
188 (Fig. 2 and Table S5). Therefore, it was likely each compound inhibited pp28
189 production by a different mechanism. Each was a potent inhibitor of several
190 kinase proteins from several groups, except for SB-220025-R, which was a
191 potent inhibitor of only 2 kinase proteins: CK1 α and p38 α (Fig. 2 and Table S5).

192 Kinase inhibition of compounds assigned z-scores of greater than 2 was
193 also examined. GW575808A and GW627512B had similar kinase selectivity
194 profiles and were inhibitors of several TK and S-T-PK group kinases (Fig. 2 and
195 Table S5). As inhibition of these TK and S-T-PK kinases can result in either
196 positive or negative z-scores (Fig. 2 and Table S5), it was unlikely that inhibition
197 of these TK and S-T-PK kinase proteins had a direct effect on pp28 production.
198 Moreover, we found that GW874091X was not a potent inhibitor of any kinase
199 assayed (Fig. 2 and Table S5). Therefore, GW874091X was either an inhibitor of
200 kinase proteins not assayed in the kinase selectivity data or exerted an effect on
201 pp28 production that did not involve inhibition of cellular kinase proteins. It,
202 therefore, remains unclear from this analysis which kinase proteins should not be
203 targeted in the development of future anti-HCMV drugs.

204 We further considered the polypharmacology of compounds tested in our
205 screen. It has been reported that ATP-competitive kinase inhibitors can inhibit the

206 function of proteins other than kinases, including aminergic GPCRs [6]. GPCR
207 agonism and antagonism of the compounds in the GSK PKIS collection has been
208 investigated elsewhere [7]. No compound within the GSK PKIS collection is a
209 GPCR agonist, but several are GPCR antagonists [7]. However, we observed no
210 correlation between compounds judged to be cytotoxic, compounds assigned a
211 z-score and GPCR antagonism (data not shown).

212

213 **Inhibition of HCMV replication by SB-734117.** We chose to focus our
214 studies on SB-734117, a compound from the furazan benzimidazole chemotype
215 that had a low z-score in our screen (Figs. 1(c) and 1(d)). First, we used viral
216 yield reduction assays to assess the ability of SB-734117 to inhibit replication of
217 HCMV strain AD169 compared to the frontline anti-HCMV drug ganciclovir (GCV)
218 (Table 2, experiment 1) at up to 96 h.p.i. The 50% effective dose (ED₅₀) of both
219 SB-734117 and GCV was 0.5 μ M, indicating that SB-734117 inhibit AD169
220 replication as efficiently as the current frontline anti-HCMV drug. To complement
221 and confirm this data we analyzed AD169 replication over time and found an
222 approximately 2-fold decrease in AD169 replication from 72-96 h.p.i. in the
223 presence of 1 μ M SB-734117 (Fig. 3(a)).

224 We also found that SB-734117 could inhibit replication of a ganciclovir
225 resistant virus (AD169-P53) and a low passage HCMV strain
226 (Merlin(RCMVR1111)), whose genomic content is similar to a clinical sample
227 [13], at low or sub-micromolar ED₅₀ values (Table 2, experiments 2 and 3,

228 respectively) at up to 96 h.p.i.. Therefore, SB-734117 was an effective inhibitor of
229 different HCMV strains.

230 To ensure that the anti-HCMV activity of SB-734117 was not due to
231 cellular cytotoxicity we used an MTT dye-uptake assay to assess cell viability and
232 cell division in uninfected cells in the presence of SB-734117. We found that the
233 50% cellular cytotoxicity (CC50) of SB-734117 after 96 hours treatment with SB-
234 734117 was greater than 10 μ M (data not shown). Thus, the CC50 values in
235 uninfected cells were greater than 10 μ M at the ED50 values for all HCMV strains
236 tested. Therefore, inhibition of HCMV replication by SB-734117 observed in
237 experiments shown in Table 2, or in the other experiments presented here, was
238 unlikely to be the result of cellular cytotoxicity or inhibition of cell division.

239

240 **Examination of HCMV immediate early protein and mRNA production**
241 **in HCMV infected cells treated with SB-734117.** We next sought to understand
242 how HCMV replication was inhibited by SB-734117. Therefore, western blotting
243 was used to analyze the accumulation of HCMV proteins in the presence or
244 absence of SB-734117 (Fig. 3(b)). Compared to treatment of infected cells with
245 DMSO (Fig. 3(b), lanes 2-4), the treatment of infected cells with SB-734117 (Fig.
246 3(b), lanes 5-7) reduced the accumulation of immediate early proteins IE1 and
247 IE2, and IE2 proteins expressed late in infection (IE2-60 and IE2-40 [14]). In this
248 and subsequent western blots the amount of β -actin in each sample was also
249 assayed, which demonstrated equivalent loading of samples in each lane.

250 We then quantified the relative density of the western blotting bands
251 shown in Fig. 3(b), by determining the band intensity of bands corresponding to
252 viral proteins relative to the intensity of the β -actin band in the same lane (Fig.
253 3(c)). We found an approximately 2-4 fold decrease in the accumulation of IE1 in
254 the presence of 1 μ M SB-734117, which is consistent with an ED50 of 0.5-1 μ M
255 shown in Table 2. The loss of IE2 protein production (approximately 2- to 20-fold,
256 depending on which antibody was used (Fig. 3(c))) was greater than IE1.
257 Consistent with loss of IE protein production and our screening results, we also
258 observed using western blotting that treatment of cells with SB-734117 resulted
259 reduced accumulation of the HCMV early and late proteins UL44 and pp28,
260 respectively, compared to infected cells treated with DMSO (data not shown). To
261 compliment these findings we assayed for differences in IE1 and IE2 mRNA
262 expression in infected cells treated with SB-734117 compared to infected cells
263 treated with DMSO using quantitative PCR against the two major IE RNA species
264 (Fig. 3(d)). This analysis revealed that no obvious defect in IE1 mRNA levels was
265 evident in the presence of SB-734117. The analysis of IE2 mRNA again did not
266 show any overt phenotype although typically a 2 fold reduction in IE2 mRNA was
267 observed in SB-734117 treated cells when compared with DMSO control.
268 However, taken together the data suggest that the decrease in IE1 and IE2
269 protein production shown in Figs. 3(b) and 3(c) was unlikely to be the result of
270 decreased *IE* gene expression.

271 Our studies thus far could not rule out that SB-734117 impacted events
272 occurring prior to IE gene expression. Thus we addressed whether the presence

273 of SB-734117 may affect virus entry into the cell or translocation of the HCMV
274 genome to the nucleus. Pre-exposure of cells to SB-734117 before infection or
275 incubation of virus with SB-734117 before infection did not increase the inhibitory
276 effects of the compound (data not shown). However, when we treated AD169
277 infected HFF cells with 1 μ M SB-734117 at 24 h.p.i. we found a 2-fold decrease in
278 HCMV replication at 120 h.p.i., compared to infected cells treated with DMSO at
279 24 h.p.i. (Fig. 4(a)). Quantitative analysis of western blotting of infected cells
280 treated as described above (Figs 4(a) and 4(b)) showed that, similar to data
281 presented in Fig. 3, treatment of infected cells with SB-734117 resulted in
282 approximately 2-fold decrease in IE2 protein production depending on which
283 antibody was used. However, there was no obvious decrease in production of
284 IE1 protein.

285 Therefore, SB-734117 had no obvious effect on cells or virus before
286 infection, but could inhibit HCMV replication after entry of the HCMV genome and
287 did so by reducing IE2 protein production. Thus, SB-734117 may not inhibit
288 events during infection before expression of IE proteins, but could have inhibitory
289 effects on HCMV replication after the initiation of IE protein production.

290

291 **Inhibition of AGC and CMCG kinase proteins by SB-734711.** Next, we
292 investigated what kinases proteins are inhibited by SB-734117. SB-734117 has
293 been reported to inhibit MSK1 [15]. However, using the kinase selectivity data
294 shown in Fig. 2 and Table S5, we found that at SB-734117 inhibits several AGC
295 kinase group proteins, including MSK1 (MSK1, MSK2, RSK1, RSK2, RSK3,

296 p70S6K1, PCK- η , PRKG2, ROCK1, ROCK2), and several CMCG kinase group
297 proteins (GSK3A, GSK3B, DYRK1A and DYRK1B). However, in our screen
298 potent and selective inhibitors of GSK3A and GSK3B had no obvious negative
299 effect on pp28 production (Table S5) and compounds with either positive or
300 negative z-scores were potent inhibitors of PKC- η , PRKG2, ROCK1 and ROCK2
301 (Table S5). Therefore, inhibition of these kinases proteins may not be related to
302 inhibition of pp28 production. Rather, analysis of SB-734117 kinase selectivity
303 data compared to other assigned z-scores argued that potent inhibition of MSK1,
304 MSK2, RSK1, RSK2, RSK3, p70S6K1, DYRK1A and DYRK1B was related to
305 inhibition of pp28 production.

306 A kinase inhibitor that is structurally unrelated to SB-734117, H-89, inhibits
307 a similar range of AGC and CMCG kinase proteins [16]. We found that H-89
308 inhibited productive HCMV replication and immediate-early protein production
309 (data not shown). Therefore, inhibition of AGC and CMCG kinase proteins, not
310 an unknown function of SB-734117, is likely to be responsible for the observed
311 defects in HCMV replication and protein production. Furthermore, using western
312 blotting [17], we found that SB-734117 did not inhibit autophosphorylation of the
313 HCMV encoded kinase UL97 (data not shown). Therefore, the anti-HCMV effects
314 of SB-734117 were unlikely to be due to inhibition of UL97.

315

316 **Analysis of CREB and histone H3 phosphorylation in HCMV infected**
317 **cells.** We then considered how inhibition of AGC and CMCG kinase proteins by
318 SB-734114 would affect post-translational modification of cellular proteins

319 thought to be involved in HCMV replication. We focused our investigation on
320 phosphorylation of the cellular transcription factor CREB and histone H3.

321 CREB is thought to directly or indirectly facilitate transcription from the
322 MIEP [18, 19] and other viral promoters [20] during productive HCMV replication
323 and it has been reported that phosphorylation of CREB at serine residue 133
324 (CREB-Ser133) by MSK1 is involved in promoting changes to chromatin required
325 for activation of the MIEP during HCMV reactivation from latency [21]. In
326 preliminary experiments we could not detect either total cellular CREB or CREB-
327 Ser133 before 72 h.p.i. using western blotting (data not shown). However, both
328 proteins could only be detected at 72 h.p.i. when we increased the amount of cell
329 lysate assayed (see Materials & Methods). Therefore, we used western blotting
330 to assay total cellular CREB and CREB-Ser133 phosphorylation in HCMV
331 infected cells treated with either DMSO or SB-734117 at 72 h.p.i. (Fig. 5(a)). We
332 observed a decrease in accumulation of CREB-Ser133 and an increase in the
333 accumulation of CREB in the presence of SB-734117 (Fig. 5(a), lane 5),
334 compared to infected cells treated with DMSO (Fig. 5(a), lane 3). Analysis of
335 relative band intensities (Fig. 5(b)), indicated that there was approximately a 2-
336 fold decrease in CREB-Ser133 in infected cells treated with SB-734117,
337 compared to those treated with DMSO and a modest increase in CREB. The 2-
338 fold decrease in the accumulation of CREB-Ser133 in the presence of 1 μ M SB-
339 734117 was consistent with the observed ED50 of 0.5-1 μ M and 2-4 fold
340 decrease in production of immediate-early HCMV protein production (Table 2
341 and Fig. 3). Therefore, the effect of SB-734117 on HCMV replication correlated

342 with a loss of CREB-Ser133 phosphorylation. Similar observations were made
343 when infected cells were treated with H89 (data not shown), indicating the AGC
344 and CMCG kinase proteins were involved in phosphorylation of CREB.

345 Phosphorylation of histone H3 by MSK1 or another kinase, IKK α is
346 required for binding of transcription factors to DNA in uninfected cells [22, 23].
347 We have previously demonstrated that phosphorylation of histone H3 at serine
348 residue 10 (H3S10p) by IKK α is associated with immediate-early protein
349 production during productive HCMV replication [17]. Also, it has been
350 demonstrated that H3S10 phosphorylation by MSK1 is associated with
351 immediate-early gene expression during reactivation of HCMV from latency [21].
352 We decided to assay H3S10 phosphorylation in the presence of SB-734117.
353 Using western blotting we analyzed accumulation of H3 and H3S10
354 phosphorylation in uninfected HFF cells (Fig. 5(c), lane 1) and AD169 infected
355 HFF cells treated with either DMSO or SB-734117 (Fig. 5(c), lanes 2-4 and 5-7,
356 respectively, at 24-72 h.p.i.). Similar levels of H3 were found in each sample,
357 however, over time we observed a decrease in H3S10p in infected cells treated
358 with SB-734117 to near undetectable levels, compared to infected cells treated
359 with DMSO. Therefore, inhibition of H3S10 phosphorylation during productive
360 HCMV replication may have contributed to the anti-HCMV activity of SB-734117.
361 Similar results were found when infected cells were treated with H89 (data not
362 shown), indicating that AGC and CMCG kinase proteins were involved in
363 phosphorylation of H3S10.

364 Phosphorylation of histone H3 at serine residue 28 (H3S28) by MSK1 is
365 also known to be associated with gene expression in uninfected cells [22]. We
366 also used western blotting to investigate H3S28 phosphorylation during HCMV
367 replication. However, we could not detect H3S28p in either uninfected HFF cells,
368 AD169 infected HFF treated with either DMSO or SB-734117, or uninfected HFF
369 cells treated with either anisomycin, which can stimulate H3S28 phosphorylation,
370 or phosphatase inhibitor okadaic acid, which can prevent dephosphorylation of
371 histones (data not shown). Therefore, we suggest that inhibition of H3S28
372 phosphorylation did not contribute to the anti-HCMV activity of SB-734117.

373

374 **Analysis of histone H3 post-translational modifications in HCMV**
375 **infected cells.** H3S10 phosphorylation by either MSK1 or IKK α is associated
376 with the presence of acetyl modifications of H3, including at acetylation (ac) of
377 lysine 14 (H3K14ac) [24-26]. There is a relationship during transcriptional
378 activation between the presence of H3S10p and H3K14ac and the association of
379 transcription factors with DNA [23, 27]. As the presence of H3K14ac is
380 associated with transcriptional activation in HCMV infected cells [28], H3K14ac
381 may be required for HCMV replication. We have previously demonstrated that
382 during HCMV replication inhibition or depletion of IKK α leads to loss of total
383 cellular H3S10 phosphorylation, but not loss of total cellular H3K14ac [17]. Thus,
384 we assayed whether treatment of HCMV infected cells by SB-734117 would lead
385 to loss of H3S10p or H3K14ac. We used western blotting to assay total cellular
386 levels of H3, H3S10p and acetylation of H3 on a number of commonly studied H3

387 lysine residues including K14 (H3K9ac, H3K14ac, H3K18ac, H3K27ac) in either
388 uninfected HFF cells (Fig. 5(c), lane 1) or HFF cells infected with HCMV and
389 treated with either DMSO or SB-734117 (Fig. 5(c), lanes 2-4 and 5-7,
390 respectively). Treatment of infected cells with SB-734117 had a slight effect (less
391 than 2-fold (data not shown)) on accumulation of H3K14ac and no detectable
392 effect on detection of H3K9ac, H3K18ac, or H3K27ac. Therefore, treatment of
393 infected cells with SB-734117 was associated with loss of total cellular H3S10p,
394 but not loss of the total cellular H3 acetylation modifications we assayed,
395 including H3K14ac.

396 The relationship between H3S10p and dimethylation (me₂) and
397 trimethylation (me₃) of H3 and H3 phosphorylation is not well characterized, but
398 it has been reported that in a murine model there is a relationship between the
399 presence of H3S10p and the presence of H3K36me₃ [29] and in *Drosophila*
400 *melanogaster* loss of the MSK1/2 homologue JIL-1 results in loss of H3S10p, H3
401 acetylation and H3 methylation, including H3K36me₃ [30]. Therefore, we asked if
402 loss of total cellular H3S10p in HCMV infected cells was associated with me₂
403 and me₃ modification of H3 lysine residues. Western blotting was used to assay
404 the presence of H3 and H3S10p, plus me₂ (H3K4me₂, H3K27me₂, H3K36me₂)
405 or me₃ (H3K4me₃, H3K9me₃, H3K27me₃, H3K36me₃) modifications of H3 in
406 uninfected HFF cells (lane 1, Figs. 5(d) and 5(e), respectively) or HFF cells
407 infected with HCMV and treated with either DMSO or SB-734117 (lanes 2-4 and
408 5-7, Figs. 5(d) and 5(e), respectively). We observed that SB-734117 had no
409 effect on total cellular accumulation of any me₂ modification of H3 (Fig. 5(d)) or

410 accumulation of H3K4me3, H3K9me3 or H3K27me3 (Fig. 5(e)). However, we
411 observed a near total loss of detectable H3K36me3 over time in infected cells
412 treated with SB-734117 (Fig. 5(e), lane 7) compared to infected cells treated with
413 DMSO (Fig. 5(e), lane 4). Similarly, a near total loss of detectable H3K36me3
414 was observed in infected cells treated with H89 (data not shown), suggesting that
415 loss of H3K36me3 is related to inhibition of AGC and CMCG kinase proteins.
416 Thus, inhibition of H3K36me3 was associated with loss of total cellular H3S10p
417 and was likely the result of inhibition of AGC and CMCG kinase proteins inhibited
418 by SB-734117. Loss of both total cellular H3S10p and total cellular H3K36me3
419 may have contributed to the anti-HCMV activity of SB-734117.

420

421 **Investigation of HCMV MIEP transcriptional activation.** Loss of CREB
422 and H3S10 phosphorylation (Figs. 5(a)-(e)) suggested that SB-734117 acted by
423 inhibiting activation of the HCMV MIEP. However, our analysis of IE1 and IE2
424 gene expression (Fig. 3(d)) indicated that transcription from the MEIP was not
425 obviously compromised in the presence of SB-734117. To investigate this in
426 more detail we utilized chromatin immunoprecipitation (ChIP) to assay the
427 presence of H3K14ac, a marker of MIEP transcriptional activation [28], at the
428 MIEP in the presence of either DMSO or SB-734117 (Fig. 6). The data showed
429 that no overt impact on H3K14ac at the MIEP between 24-72hpi in DMSO or SB-
430 734117 treated cells. Indeed, we noted that SB-734117 treated cells actually
431 showing higher levels of H3K14ac at the MIEP at late times post infection when
432 compared to control. Therefore, in agreement with our analysis of IE1 and IE2

433 gene expression (Fig. 3(d)), there was no obvious defect in MIEP transcriptional
434 activation in the presence of SB-734177. Thus, the observed defects in HCMV
435 immediate-early protein production (Figs 3 and 4) could not be explained by
436 defects in transcription from the MIEP.

437

438

439 **DISCUSSION**

440

441 Our overall analysis of the chemotypes screened indicated that each
442 chemotype contained compounds with anti-HCMV activity, however modest that
443 anti-HCMV activity may have been. As the structure of each compound in each
444 chemotype is known, structure-activity relationships derived from our data could
445 form the basis of future studies in the discovery of compounds with anti-HCMV
446 activity from each chemotype.

447 Our survey of the GSK PKIS kinase selectivity data argued that several
448 proteins from several kinase groups, alone or in combination, were required for
449 pp28 production. These proteins kinases include those from the STE (including
450 MAP4K4 and MNK), CAMK (including PRKD1, PRKD2 and PRKD3) and CMCG
451 (including CLK2, HIPK1, HIPK4, DYRK1A, DYRK1B, DYRK2) kinase groups.
452 The function of these protein kinases in productive HCMV replication is unclear
453 or unknown. Therefore, it is possible that our data identified novel cellular factors
454 required for productive HCMV replication. However, the polypharmacology of the
455 compounds tested makes it difficult to identify specific kinases required for
456 productive HCMV replication. Thus, each of the aforementioned kinases will have
457 to be tested individually to identify their roles in HCMV infected cells. With this
458 information these kinases could be exploited as novel anti-HCMV drug targets.

459 We chose to pursue studies of SB-734117 as this compound had one of
460 the greatest negative effects on pp28 production in our screen, with no obvious
461 cytotoxic effects, and was an effective inhibitor of a number of HCMV strains.

462 Moreover, the function of the AGC and CMCG kinase proteins inhibited by SB-
463 734117 in productive HCMV replication was unknown or unclear.

464 SB-734117 was originally described as an inhibitor of MSK1 [15].
465 However, like other MSK1 inhibitors [16], SB-734117 displays polypharmacology
466 and can inhibit several kinases whose roles in productive HCMV replication are
467 unknown or unclear. Thus, to understand how SB-734117 inhibits HCMV
468 replication it will be necessary to understand if a particular kinase or a
469 combination of kinase proteins is required for productive HCMV replication. A
470 truly selective inhibitor of MSK1 has yet to be found. Structure-activity
471 relationships involving SB-734117 and other furazan benzimidazole compounds
472 could be explored to generate compounds with improved anti-HCMV activity and
473 kinase selectivity. However, we could discern no obvious relationship between
474 inhibition of HCMV replication, kinase selectivity and the structures of
475 compounds within the furazan benzimidazole chemotype analyzed here due to
476 the small number of furazan benzimidazole compounds that returned low
477 negative z-scores in our screen (data not shown). An improved compound
478 related to SB-734117 would have value as an anti-HCMV drug, as it would have
479 the potential to inhibit both productive HCMV replication and reactivation of
480 HCMV from latency. Plus, based on our observations, an improved compound
481 should be as effective an inhibitor of HCMV replication as ganciclovir and be able
482 to inhibit replication of ganciclovir resistant HCMV strains.

483 Perhaps the most intriguing observations we make concern modification of
484 histone H3 in the presence of SB-734117. Previous observations from our

485 laboratory have indicated that IKK α was required for H3S10 phosphorylation in
486 AD169 infected HFF cells [17], which is consistent with data presented
487 elsewhere indicating that H3S10 is substrate of IKK α [24, 25, 31-33]. We note
488 that inhibition of IKK α results in loss of H3S10p early in HCMV replication (24
489 h.p.i. onwards) [17], whereas treatment with SB-734117 leads to a loss of
490 H3S10p later in HCMV replication (48-72 h.p.i.). SB-734117 does not inhibit
491 IKK α (Table S5). Therefore, we propose that in HCMV infected cells a
492 mechanism exists wherein IKK α does not phosphorylate H3S10 during treatment
493 with SB-734117. Conversely, kinases inhibited by SB-734117 do not
494 phosphorylate H3S10 when IKK α is inhibited or depleted. This mechanism may
495 ensure appropriate regulation of H3S10 phosphorylation that is necessary for
496 productive HCMV replication.

497 It has been reported that in uninfected cells from humans and mice loss of
498 H3S10p can lead to loss of H3K14ac [24-26]. However, we did not observe loss
499 of total cellular H3K14ac upon treatment of HCMV infected cells with SB-734117
500 or in our previous study where inhibition or depletion of IKK α resulted in loss of
501 H3S10p [17]. We speculate, as we have done previously [17], that an as yet
502 unrecognized mechanism exists in HCMV infected cells that maintains total
503 H3K14ac when total H3S10p levels are lowered to near undetectable levels.

504 We observed that treatment of HCMV infected cells with SB-734117
505 resulted in loss of H3K36me3. We have previously found that depletion of IKK α
506 in HCMV infected cells leads to loss of H3S10p, but not H3K36me3 [17].
507 Therefore, the loss of H3K36me3 in HCMV infected cells is related to loss of

508 H3S10p during inhibition of AGC and CMCG kinases, but not during inhibition of
509 IKK α . This may be related to regulation of H3S10 phosphorylation by different
510 kinases, as we discuss above. We propose that, as in mice and *Drosophila* [29,
511 30], the presence of H3K36me3 in HCMV infected cells is related to the presence
512 of H3S10p, potentially via phosphorylation of H3 by MSK1. Alternatively, there
513 may be a substrate of kinase proteins inhibited by SB-734117 whose
514 phosphorylation directly or indirectly mediates H3K36 tri-methylation.

515 Treatment of HCMV infected cells with SB-734117 impacted on immediate
516 early protein production and caused loss of total cellular levels of post-
517 translational modification of cellular factors potentially involved in transactivation
518 of the HCMV MIEP. However, in the presence of SB-734117 we did not find
519 obvious defects in activation of transcription from the HCMV MIEP or defects in
520 immediate-early gene transcription. Therefore, the loss of total cellular levels of
521 CREB and H3S10 phosphorylation or H3K36me3 had no direct impact on
522 transcription from the HCMV MIEP. This interpretation would be consistent with
523 previous studies that have shown that the deletion of CREB binding sites from
524 the MIEP has little impact on productive HCMV replication [21, 34]. During
525 reactivation, it is hypothesized the H3S10p is important as it drives the transition
526 of the MIEP from a repressed to active promoter, a mechanism also proposed for
527 HSV reactivation [35] Thus, during productive HCMV replication at high MOI,
528 where the MIEP is associated with active, not repressed, chromatin very early
529 post infection [28], H3S10p may not be essential for transcription. However, it
530 remains possible that H3S10p has a role in the release of Early and Late HCMV

531 promoters from repression as infection proceeds. Thus, future challenges will
532 include mapping of CREB, H3S10p and H3K36me3 to viral and cellular
533 promoters to understand in more detail to understand their possible involvement
534 in productive HCMV replication.

535 We propose that the greatest impact of SB-734117 on productive HCMV
536 replication is on production of IE proteins. It will be important to investigate if SB-
537 734117 impacts on additional phosphorylation events that are required for
538 production of both proteins. Post-translational modification of both IE1 and IE2 is
539 not yet completely characterized. Thus, SB-734117 could directly or indirectly
540 inhibit phosphorylation of these proteins, which leads to their loss. Further
541 investigation of IE protein production and the roles of IE post-translational
542 modification are required in order to fully understand the mechanism of action of
543 SB-734117 during productive HCMV replication.

544

545 **MATERIALS & METHODS**

546

547 **Compounds.** The GSK PKIS library (version 1) was supplied to the Institute of
548 Chemistry and Chemical Biology-Longwood at Harvard Medical School by GSK.
549 SB-734117 was a kind gift from GlaxoSmithKline. Ganciclovir was obtained from
550 SIGMA. H89 and heparan sulphate were obtained from Calbiochem. All drugs
551 were resuspended in dimethyl sulfoxide (DMSO).

552

553 **Cells and viruses.** Human foreskin fibroblast (HFF) cells (clone Hs29) were
554 obtained from American Type Culture Collection no. CRL-1684 (ATCC,
555 Manassas, VA) and maintained in Dulbeccos Modified Eagles Medium (DMEM)
556 (Gibco) containing 5% fetal bovine serum (FBS) (Gibco), plus penicillin and
557 streptomycin. High passage HCMV strain AD169 was a gift from Don Coen
558 (Harvard Medical School). Low passage strain Merlin R1111 (derived from
559 BACmid pAL1111, which does not express RL13 and UL128)[36] was a gift from
560 Richard Stanton (Cardiff University). Ganciclovir resistant virus AD169-P53 was
561 supplied by the National Institute of Health (NIH) AIDS Reagent Program.

562

563 **Screening of GSK PKIS collection and analysis of screening data.** See
564 supplementary material.

565

566 **Characterization of compounds within the GSK PKIS collection.** See
567 supplementary material.

568

569 **Viral yield reduction assays.** Assays were performed essentially as described
570 in [37]. HFF cells were plated at 5×10^4 cells per well in 24-well plates. After
571 overnight incubation, cells were infected with HCMV at a multiplicity of infection
572 (MOI) of 1. After virus adsorption for 1 hour at 37°C, cells were washed and
573 incubated with 0.5 ml of media containing DMSO or compounds at a range of
574 concentrations in duplicate. Plates were incubated for 4 days at 37°C. Titers
575 were determined by serial dilution of viral supernatant onto HFF monolayers
576 which were covered in DMEM containing 5% FBS, 0.6% methylcellulose and
577 antibiotics. Cultures were incubated for 14 days, cells were stained, with crystal
578 violet and plaques were counted. Data shown represents the mean value of
579 duplicate plaque counts. The final concentration of DMSO in all samples was
580 maintained at <1% (v/v).

581

582 **MTT cytotoxicity assays.** Assays were performed essentially as described [37].
583 HFF cells were seeded at 1×10^4 cells per well into 96-well plates. After
584 overnight incubation to allow cell attachment, cells were treated for the time
585 indicated in the text with at range of concentrations concentrations in duplicate.
586 The highest concentration of compound tested was 10 μ M. Cell viability was then
587 determined with an MTT assay according to the manufacturer's instructions (GE
588 Healthcare). Data shown represents the mean value of duplicate readings. The
589 final concentration of DMSO in all samples was maintained at <1% (v/v). As a

590 positive control, in all experiments a 2-fold dilution series of HFF cells starting at
591 1×10^4 cells per well was included. In each experiment we found a linear
592 relationship between the number of cells per well and output from the MTT assay
593 (data not shown).

594

595 **Western blotting.** At time points indicated in the text cells were washed
596 once with PBS and resuspended in 100 μ l Laemmli buffer containing 5% β -
597 mercaptoethanol. Proteins were separated on 8% or 10% polyacrylamide gels.
598 Typically, a volume of cell lysate corresponding to 1×10^4 HFF cells was
599 analyzed, except when blotting for CREB or CREB-Ser133 when a volume of cell
600 lysate corresponding to 5×10^5 HFF cells was analyzed. Antibodies used are
601 listed in the supplementary material. Relative band intensity (band intensity
602 relative to β -actin signal in the same lane) was analyzed using ImageJ software,
603 obtained from the National Institutes of Health (USA).

604

605 **RNA analysis and Quantitative PCR.** Quantitative PCR was performed
606 using a SYBR green qPCR kit (Qiagen) and analysed using the $\Delta\Delta$ CT method to
607 compare DMSO versus SB-734117 treated cells. Briefly, cDNA was prepared
608 from RNA extracted from infected cells at timepoints indicated in the Figure.
609 cDNA and no RT controls were amplified in technical duplicates from multiple
610 experiments using a constant primer in exon 3 (UL122-123) and a primer from

611 exon 4 (UL123) or exon 5 (UL122). Cellular RNA was amplified using 18S RNA
612 primers.

613 Exon 3: ACG AGA ACC CCG AGA AAG ATG; exon 4: CGC CAG TGA ATT
614 TCT CTT C; exon 5: CCG GGG AGA GGA GTG TTA GT; 18S for: GTA ACC
615 CGT TGA ACC CCA; 18S rev: CCA TCC AAT CGG TAG TAG CG.

616 qPCR was performed using cycling conditions: 95°C (15s) then 40 cycles of 94°C
617 (15s), 55°C (30s) and 72°C (30s).

618

619 **Chromatin immunoprecipitation.** All procedures were performed
620 essentially as previously described [21]. Briefly, HFFs were fixed with 1%
621 formaldehyde (10 mins) and then enzymatically digested to fragment DNA as
622 described by manufacturer (Pierce chromatin preparation kit). DNA associated
623 with histones was immunoprecipitated with control serum (Sigma) or anti-acetyl-
624 histone H3-lysine 14 (1:150 dilution of antibody – see supplementary material).
625 For detection of the HCMV MIEP, DNA from disrupted nucleosomes was
626 precipitated and amplified by SYBR green qPCR kit (Qiagen) using 5' - TGG
627 GAC TTT CCT ACT TGG (sense) and 5' - CCA GGC GAT CTG ACG GTT (anti-
628 sense) primers. Specific immuno-precipitation of sequences was expressed as
629 enrichment from Input.

630

631 **ACKNOWLEDGMENTS**

632

633 We would like to express our thanks to Don Coen for his encouragement during
634 this study and his support of BLS through grants awarded to DC from the
635 National Institutes of Health (R01 AI019838 and R01 AI026077). This work was
636 also supported by New Investigator funds from St George's, University of
637 London, a St George's Impact & Innovation Award and a PARK/WestFocus
638 Award (all to B.L.S.). M.J.M. is supported by a Medical Research Council (UK)
639 PhD studentship. We also acknowledge Simon Arthur, Nathanael Gray,
640 GlaxoSmithKline, Gloria Komazin-Meredith, Andrew Macdonald and Richard
641 Stanton for providing reagents and insightful discussions, plus l'ah Z Donovan-
642 Banfield for technical assistance and Lisa Rickelton for assistance with
643 preparation of figures. Special thanks go to all members of Institute of Chemistry
644 and Chemical Biology-Longwood for their assistance in all aspects of the
645 screening process.

646

647 **ABBREVIATIONS**

648

649 **AGC**: containing PKA, PKG, PKC families group, **CAMK**: calcium/calmodulin-
650 dependent protein kinase group, **CDK**: cyclin-dependent kinase, **CLK2**: cyclin-
651 dependent kinase-like kinase 2, **CK**: casein kinase, **CMCG**: containing CDK,
652 MAPK, GSK3, CLK families group, **CREB**: cAMP response element-binding
653 protein, **GCV**: ganciclovir, **DYRK**: dual-specificity tyrosine phosphorylation-
654 regulated kinase, **GSK**: glycogen synthase kinase, **HCMV**: human
655 cytomegalovirus, **HIPK**: homeodomain interacting protein kinase, **MAPK4K4**:
656 mitogen-activated protein kinase kinase kinase 4, **MNK1**: MAP kinase-
657 interacting serine/threonine-protein kinase 1, **MSK**: mitogen and stress kinase,
658 **PCK-η**: protein kinase C-η, **PLK-1**: polo-like kinase 1, **PRKD**: protein kinase D,
659 **PRKG**: protein kinase, cGMP-Dependent, **PRKX**: protein kinase, x-linked,
660 **p70S6K1**: ribosomal protein S6 kinase beta-1, **ROCK**: rho-associated, coiled-
661 coil-containing protein kinase 1, **RSK**: ribosomal s6 kinase, **STE**: homologs of
662 yeast Sterile 7, Sterile 11, Sterile 20 kinases group, **S-T-PK**: serine/threonine
663 protein kinase group, **TK**: tyrosine kinase group, **TKL**: tyrosine kinase-like group.

664

665 **REFERENCES**

666

- 667 1. **Mocarski ES, Shenk T, Griffiths PD, Pass RF.** Cytomegaloviruses In:
668 Knipe DM, Howley PM, editors. Fields Virology. 2. 6th ed. New York, NY:
669 Lippincott, Williams & Wilkins; 2015. p. 1960-2015.
- 670 2. **Krause PR, Bialek SR, Boppana SB, Griffiths PD, Laughlin CA, et al.**
671 Priorities for CMV vaccine development. *Vaccine*. 2013;32:4-10.
- 672 3. **Coen DM, Schaffer PA.** Antiherpesvirus drugs: a promising spectrum of
673 new drugs and drug targets. *Nat Rev Drug Discov*. 2003;2:278-288.
- 674 4. **Rogers N.** A dormant danger: New therapies target a ubiquitous pathogen
675 known as cytomegalovirus. *Nature medicine*. 2015;21:1104-1105.
- 676 5. **Muller S, Chaikuad A, Gray NS, Knapp S.** The ins and outs of selective
677 kinase inhibitor development. *Nature chemical biology*. 2015;11:818-821.
- 678 6. **Paolini GV, Shapland RH, van Hoorn WP, Mason JS, Hopkins AL.**
679 Global mapping of pharmacological space. *Nat Biotechnol*. 2006;24:805-815.
- 680 7. **Elkins JM, Fedele V, Szklarz M, Abdul Azeez KR, Salah E, et al.**
681 Comprehensive characterization of the Published Kinase Inhibitor Set. *Nat*
682 *Biotechnol*. 2016;34:95-103.
- 683 8. **Drewry DH, Willson TM, Zuercher WJ.** Seeding collaborations to
684 advance kinase science with the GSK Published Kinase Inhibitor Set (PKIS).
685 *Current topics in medicinal chemistry*. 2014;14:340-342.
- 686 9. **Polachek WS, Moshrif HF, Franti M, Coen DM, Sreenu VB, et al.** High-
687 Throughput Small Interfering RNA Screening Identifies Phosphatidylinositol 3-

688 Kinase Class II Alpha as Important for Production of Human Cytomegalovirus
689 Virions. J Virol. 2016;90:8360-8371.

690 10. **Compton T, Nowlin DM, Cooper NR.** Initiation of human cytomegalovirus
691 infection requires initial interaction with cell surface heparan sulfate. Virology.
692 1993;193:834-841.

693 11. **Birmingham A, Selfors LM, Forster T, Wrobel D, Kennedy CJ, et al.**
694 Statistical methods for analysis of high-throughput RNA interference screens.
695 Nature methods. 2009;6:569-575.

696 12. **Zhang JH, Chung TD, Oldenburg KR.** A Simple Statistical Parameter for
697 Use in Evaluation and Validation of High Throughput Screening Assays. Journal
698 of biomolecular screening. 1999;4:67-73.

699 13. **Wilkinson GW, Davison AJ, Tomasec P, Fielding CA, Aicheler R, et**
700 **al.** Human cytomegalovirus: taking the strain. Medical microbiology and
701 immunology. 2015;204:273-284.

702 14. **White EA, Del Rosario CJ, Sanders RL, Spector DH.** The IE2 60-
703 kilodalton and 40-kilodalton proteins are dispensable for human cytomegalovirus
704 replication but are required for efficient delayed early and late gene expression
705 and production of infectious virus. J Virol. 2007;81:2573-2583.

706 15. **Bamford MJ, Alberti MJ, Bailey N, Davies S, Dean DK, et al.** (1H-
707 imidazo[4,5-c]pyridin-2-yl)-1,2,5-oxadiazol-3-ylamine derivatives: a novel class of
708 potent MSK-1-inhibitors. Bioorganic & medicinal chemistry letters. 2005;15:3402-
709 3406.

- 710 16. **Naqvi S, Macdonald A, McCoy CE, Darragh J, Reith AD, et al.**
711 Characterization of the cellular action of the MSK inhibitor SB-747651A. The
712 Biochemical journal. 2012;441:347-357.
- 713 17. **Ho CM, Donovan-Banfield IZ, Tan L, Zhang T, Gray NS, et al.** Inhibition
714 of IKKalpha by BAY61-3606 Reveals IKKalpha-Dependent Histone H3
715 Phosphorylation in Human Cytomegalovirus Infected Cells. PloS one.
716 2016;11:e0150339.
- 717 18. **Chia YL, Ng CH, Lashmit P, Chu KL, Lew QJ, et al.** Inhibition of human
718 cytomegalovirus replication by overexpression of CREB1. Antiviral research.
719 2014;102:11-22.
- 720 19. **Stinski MF, Thomsen DR, Stenberg RM, Goldstein LC.** Organization
721 and expression of the immediate early genes of human cytomegalovirus. J Virol.
722 1983;46:1-14.
- 723 20. **Rodems SM, Clark CL, Spector DH.** Separate DNA elements containing
724 ATF/CREB and IE86 binding sites differentially regulate the human
725 cytomegalovirus UL112-113 promoter at early and late times in the infection. J
726 Virol. 1998;72:2697-2707.
- 727 21. **Kew VG, Yuan J, Meier J, Reeves MB.** Mitogen and stress activated
728 kinases act co-operatively with CREB during the induction of human
729 cytomegalovirus immediate-early gene expression from latency. PLoS
730 pathogens. 2014;10:e1004195.
- 731 22. **Arthur JS.** MSK activation and physiological roles. Frontiers in bioscience
732 : a journal and virtual library. 2008;13:5866-5879.

- 733 23. **Macdonald N, Welburn JP, Noble ME, Nguyen A, Yaffe MB, et al.**
734 Molecular basis for the recognition of phosphorylated and phosphoacetylated
735 histone h3 by 14-3-3. *Mol Cell*. 2005;20:199-211.
- 736 24. **Yamamoto Y, Verma UN, Prajapati S, Kwak YT, Gaynor RB.** Histone
737 H3 phosphorylation by IKK-alpha is critical for cytokine-induced gene expression.
738 *Nature*. 2003;423:655-659.
- 739 25. **Anest V, Hanson JL, Cogswell PC, Steinbrecher KA, Strahl BD, et al.**
740 A nucleosomal function for IkkappaB kinase-alpha in NF-kappaB-dependent gene
741 expression. *Nature*. 2003;423:659-663.
- 742 26. **Vicent GP, Ballare C, Nacht AS, Clausell J, Subtil-Rodriguez A, et al.**
743 Induction of progesterone target genes requires activation of Erk and Msk
744 kinases and phosphorylation of histone H3. *Mol Cell*. 2006;24:367-381.
- 745 27. **Lo WS, Trievel RC, Rojas JR, Duggan L, Hsu JY, et al.** Phosphorylation
746 of serine 10 in histone H3 is functionally linked in vitro and in vivo to Gcn5-
747 mediated acetylation at lysine 14. *Mol Cell*. 2000;5:917-926.
- 748 28. **Cuevas-Bennett C, Shenk T.** Dynamic histone H3 acetylation and
749 methylation at human cytomegalovirus promoters during replication in fibroblasts.
750 *J Virol*. 2008;82:9525-9536.
- 751 29. **Graff J, Woldemichael BT, Berchtold D, Dewarrat G, Mansuy IM.**
752 Dynamic histone marks in the hippocampus and cortex facilitate memory
753 consolidation. *Nature communications*. 2012;3:991.

- 754 30. **Karam CS, Kellner WA, Takenaka N, Clemmons AW, Corces VG.** 14-3-
755 3 mediates histone cross-talk during transcription elongation in Drosophila. PLoS
756 genetics. 2010;6:e1000975.
- 757 31. **Dong W, Li Y, Gao M, Hu M, Li X, et al.** IKKalpha contributes to UVB-
758 induced VEGF expression by regulating AP-1 transactivation. Nucleic Acids Res.
759 2012;40:2940-2955.
- 760 32. **Lubin FD, Sweatt JD.** The I kappa B kinase regulates chromatin structure
761 during reconsolidation of conditioned fear memories. Neuron. 2007;55:942-957.
- 762 33. **Thorne JL, Ouboussad L, Lefevre PF.** Heterochromatin protein 1
763 gamma and I kappa B kinase alpha interdependence during tumour necrosis
764 factor gene transcription elongation in activated macrophages. Nucleic Acids
765 Res. 2012;40:7676-7689.
- 766 34. **Meier JL, Keller MJ, McCoy JJ.** Requirement of multiple cis-acting
767 elements in the human cytomegalovirus major immediate-early distal enhancer
768 for viral gene expression and replication. J Virol. 2002;76:313-326.
- 769 35. **Cliffe AR, Arbuckle JH, Vogel JL, Geden MJ, Rothbart SB, et al.**
770 Neuronal Stress Pathway Mediating a Histone Methyl/Phospho Switch Is
771 Required for Herpes Simplex Virus Reactivation. Cell host & microbe.
772 2015;18:649-658.
- 773 36. **Stanton RJ, Baluchova K, Dargan DJ, Cunningham C, Sheehy O, et**
774 **al.** Reconstruction of the complete human cytomegalovirus genome in a BAC
775 reveals RL13 to be a potent inhibitor of replication. The Journal of clinical
776 investigation. 2010;120:3191-3208.

777 37. **Loregian A, Coen DM.** Selective anti-cytomegalovirus compounds
778 discovered by screening for inhibitors of subunit interactions of the viral
779 polymerase. *Chem Biol.* 2006;13:191-200.

780

781

782 **FIGURE LEGENDS**

783

784 **Fig. 1 High throughput screening of the GSK PKIS collection.** (a) Diagram of
785 screening process. (b) A representative example of a microscopy image from an
786 Image Express Micro microscope of infected HFF cells treated with Hoechst
787 33342 (blue), Deep Red Cell Mask (Red) and primary and secondary antibodies
788 to detect HCMV pp28 (green). The large white box is a magnified image of the
789 area identified by the small white box. (c) Plot of z-scores where each data point
790 represents a single compound. The compounds with highest and lowest z-scores
791 are identified and their z-scores are stated in parentheses. (d) Structures of
792 compounds with z-scores ((i)-(iv)) lower than -2 and ((v)-(vii)) greater than 2.

793

794 **Fig. 2 Kinase selectivity of compounds assigned z-scores.** The full list of
795 kinase selectivity data is shown in Table S5. Table S5 is shown here as a
796 “heatmap” of kinase selectivity wherein the potency of each compound at 1 μ M
797 concentration against a particular kinase is represented in colour as indicated at
798 the bottom of the figure (less than 0% inhibition – blue, 0-50% inhibition – green,
799 51-75% inhibition – yellow, 76-90% inhibition – orange, greater than 91%
800 inhibition – red). Each row represents a compound and each column represents
801 the kinase tested. The z-scores of each compound are indicated to the left of the
802 figure. The kinase groups of each kinase tested are indicated above the figure.
803 (a)-(c) Kinase inhibition of compounds with z-scores of less than -1 not found in

804 compounds with z-scores greater than 1. (d) Kinase inhibition of compounds with
805 z-scores greater than 1 not found in compounds with z-scores of less than -1.

806

807 **Fig. 3 Analysis of HCMV replication and protein production in infected HFF**

808 **cells treated with DMSO or SB-734117 at the time of infection.** (a) HFF cells

809 were infected at MOI1 with AD169 then treated with 1 μ M SB-734117 or the

810 equivalent volume of DMSO. Viral titre (plaque forming units (p.f.u./ml)) was

811 determined at the indicated time points (hours post infection (h.p.i.)). Data points

812 and error bars represent the mean and standard deviation, respectively, from

813 three experiments. (b) HFF cells were infected with AD169 at an MOI of 1, then

814 treated with either 1 μ M SB-734117 or the equivalent volume of DMSO. Cell

815 lysates were prepared for western blotting at the time points (hours post infection

816 (h.p.i.)) indicated above the figure. Uninfected cells harvested at the time of

817 infection are shown as 0 h.p.i.. Proteins recognized by the antibodies used are

818 indicated to the right of each figure. The positions of molecular mass markers

819 (kDa) are indicated to the left of each figure. (c) Relative band intensity of

820 immediate-early protein bands relative to β -actin signal in the same lane in

821 Figure 3A, as quantified using ImageJ. Band intensities of 0-1, 1-2 and greater

822 than 2 are highlighted in light grey, dark grey and black, respectively. (d) HFF

823 cells were infected at MOI1 with AD169 then treated with 1 μ M SB-734117 or the

824 equivalent volume of DMSO. Samples were prepared for quantitative PCR

825 analysis of *IE1* and *IE2* mRNA expression, respectively, at the time points

826 indicated in the figures. Data and error bars represent the mean and standard

827 deviation of three PCR replicates from each sample, respectively (n=2). Change
828 in gene expression relative to DMSO is shown for each timepoint using $\Delta\Delta\text{CT}$
829 method.

830

831 **Fig. 4 Analysis of HCMV replication and protein production in infected HFF**
832 **cells treated with DMSO or SB-734117 at 24 hours post infection.** (a) HFF
833 cells were infected at MOI1 with AD169 then treated with 1 μ M SB-734117 or the
834 equivalent volume of DMSO at 24 hours post infection. Viral titre (plaque forming
835 units (p.f.u./ml)) was determined at 120 hours post infection (h.p.i.). (b) HFF
836 cells were infected with AD169 at an MOI of 1, then treated with either 1 μ M SB-
837 734117 or the equivalent volume of DMSO at 24 hours post infection. Cell
838 lysates were prepared for western blotting at the time points (hours post infection
839 (h.p.i.)) indicated above the figure. Infected cells harvested at 24 h.p.i. that were
840 not treated with either SB-734117 or DMSO were also assayed. Proteins
841 recognized by the antibodies used are indicated to the right of each figure. The
842 positions of molecular mass markers (kDa) are indicated to the left of each figure.
843 (c) Relative band intensity of immediate-early protein bands relative to β -actin
844 signal in the same lane in Figure 3A, as quantified using ImageJ. Band intensities
845 of 0-1, 1-2 and greater than 2 are highlighted in light grey, dark grey and black,
846 respectively.

847

848 **Fig. 5 Inhibition of phosphorylation of cellular proteins by SB-734117** ((a),
849 (c)-(3)) HFF cells were infected with AD169 at an MOI of 1, then treated with

850 either 1 μ M SB-734117 or the equivalent volume of DMSO (as indicated above
851 each Figure). Cell lysates were prepared for western blotting at (a) 72 h.p.i. or
852 ((c)-(e)) as indicated above the figure. Uninfected cells harvested at the time of
853 infection are shown as 0 h.p.i. in (c)-(e). In (a) no lysate was analyzed in lanes 2
854 and 4. Proteins recognized by the antibodies used are indicated to the right of
855 each figure. The positions of molecular mass markers (kDa) are indicated to the
856 left of each figure. (b) Relative band intensity of CREB and CREB-Ser133 bands
857 relative to β -actin signal in the same lane in Fig. 4(a), as quantified using ImageJ.
858 Band intensities of 0-1, 1-2 and greater than 2 are highlighted in light grey, dark
859 grey and black, respectively.

860

861 **Fig. 6 H3K14ac at the MIEP is unaffected in SB-734117 treated cells.** DNA
862 was immune-precipitated from infected cells (24-72hpi) treated with either DMSO
863 or SB-734117 using an anti-H3K14ac antibody (K14) or isotype control (C), then
864 amplified in an MIEP qPCR. Enrichment of MIEP sequences was expressed
865 relative to amplification in Input sample. Data and error bars represent the mean
866 and standard deviation of three PCR replicates from each sample, respectively

867 **TABLES**

868

869 Table 1

870

Chemotype	Total no. of compounds in chemotype	No. of compounds excluded due to cytotoxicity	No. of compounds assigned z-scores.
4-pyrimidinyl ortho-aryl azoles	31	0	31
Oxindoles	30	3	27
Furazan benzimidazoles	25	1	24
4-anilino quinazolines and related	25	0	25
Benzimidazole N-thiophenes	21	9	12
4-pyridyl ortho-aryl azoles	18	0	18
2H-3 pyrimidinyl pyrazolopyridazines	16	7	9
2-amino oxazoles	15	0	15
4-hydrazinyl pyrazolopyrimidines	15	0	15
2,4-dianilino pyrrolopyrimidines	15	1	14
Biaryl amides	14	0	14
3-vinyl pyridines	13	0	13
Anilino thienopyrimidines	12	0	12
Benzimidazolyl diaryl ureas	12	2	10
2-aryl 3-pyridimidinyl pyrazolopyridazines	12	0	12
2,4-diamino pyrimidines	12	0	12
Maleimide	11	0	11
Furopyrimidines and related	9	0	9
Indazole-3-carboxamides	7	1	6
3-amino pyrazolopyridines	7	3	4
2-pyridinyl imidazoles and related	7	0	7
4-anilino 5-alkynyl pyrimidines	7	0	7
3-cyano thiophenes	6	2	4
Phenyl carboxamides	6	0	6
Indazole-5-carboxamides	6	0	6
3-amino pyrazolopyridazines	4	1	3
3-amino pyrazoles	3	0	3
Imidazotriazine	3	0	3
4-anilino quinolones	2	0	2
6-phenyl isoquinolines	2	1	1
3-benzyl pyrimidines	1	0	1

871

872

873

874 Table 2

875

Experiment	Viral Strain	Compound	ED50* (μ M)
1	AD169	SB-734117	0.5
	AD169	GCV [†]	0.5
2	AD169	SB-734117	0.4
	AD169-P53	SB-734117	1.3
3	AD169	SB-734117	1
	Merlin(RCMV11111)	SB-734117	2

876 *50% effective dose

877 [†]Ganciclovir

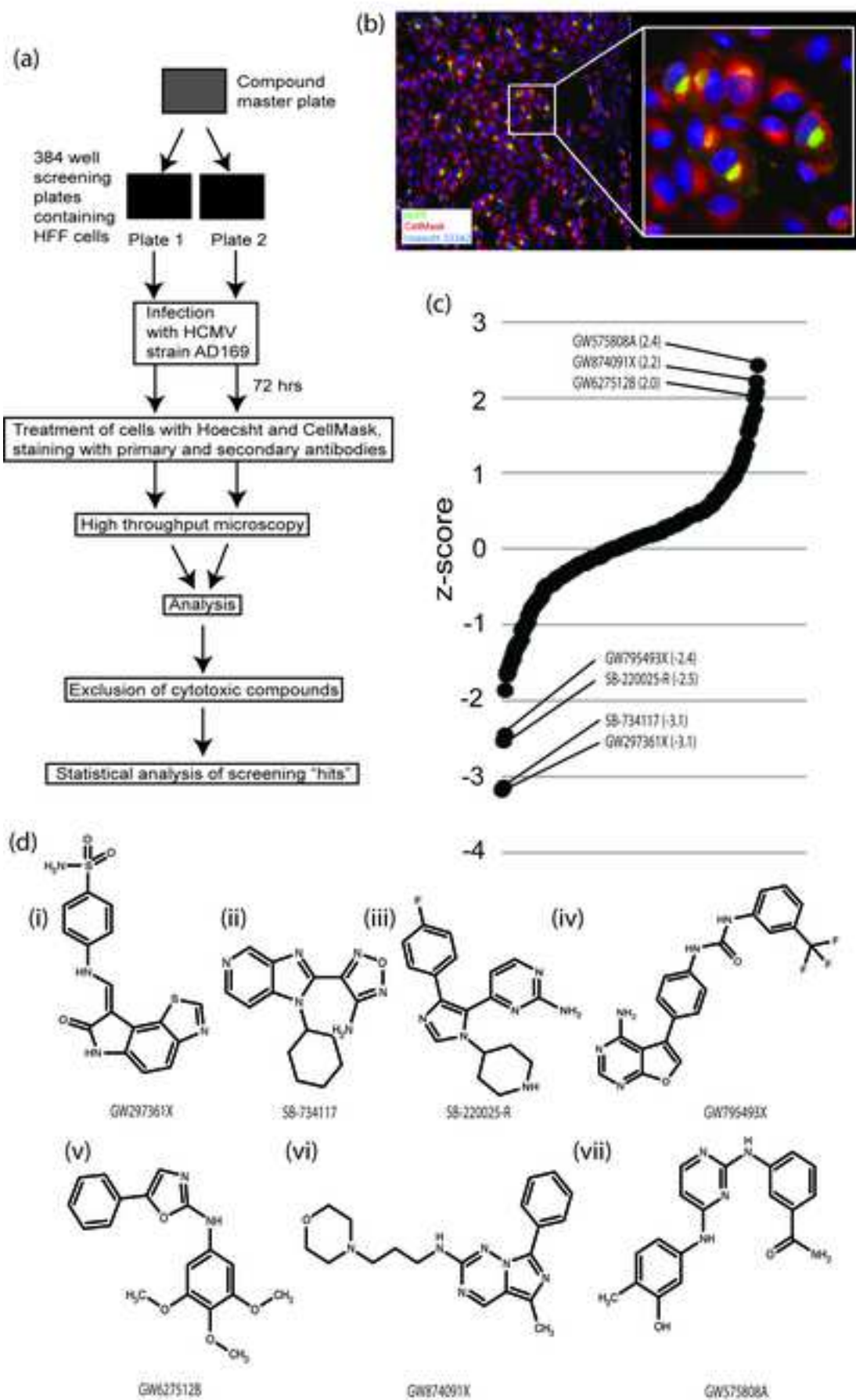


Fig. 1

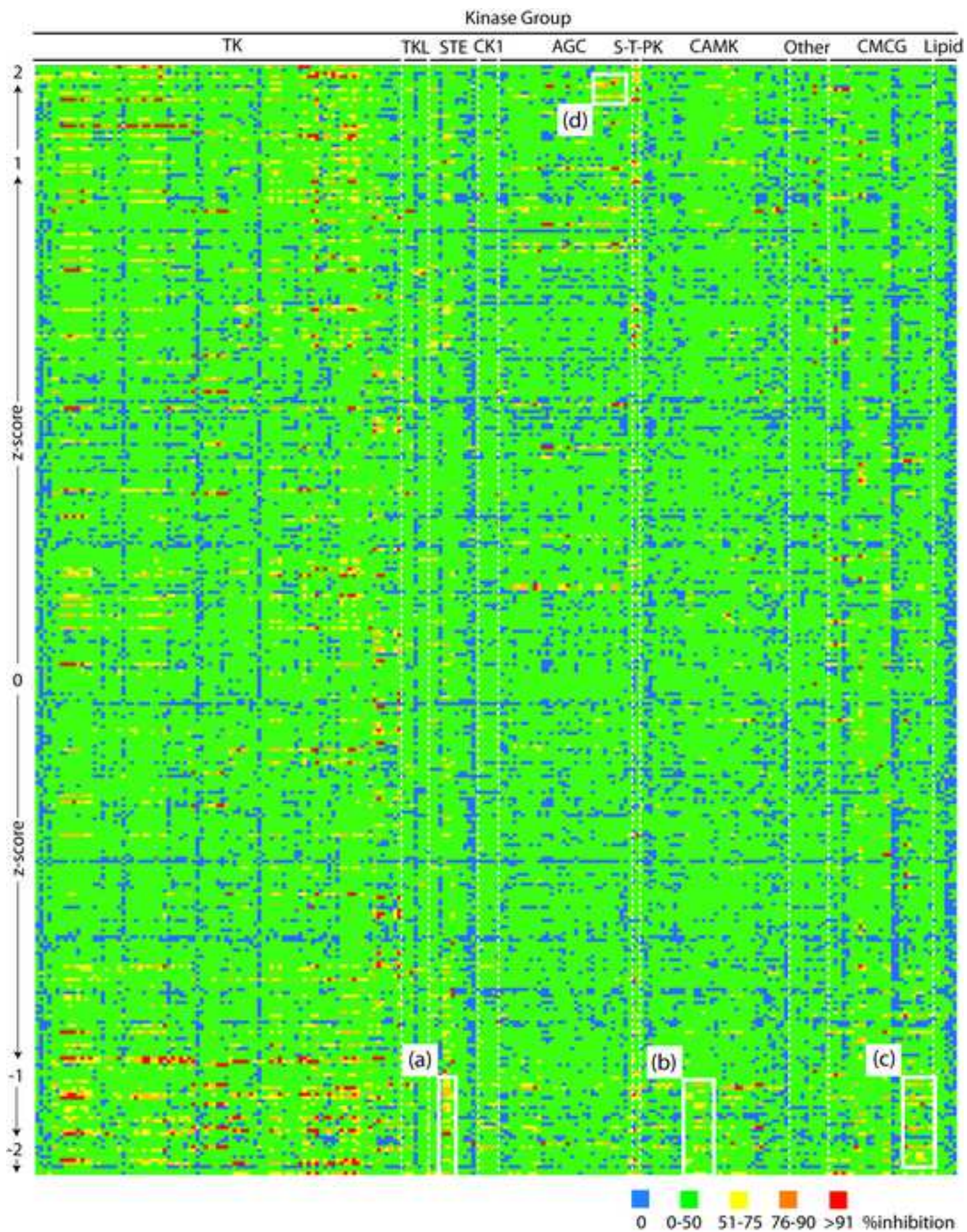


Fig. 2

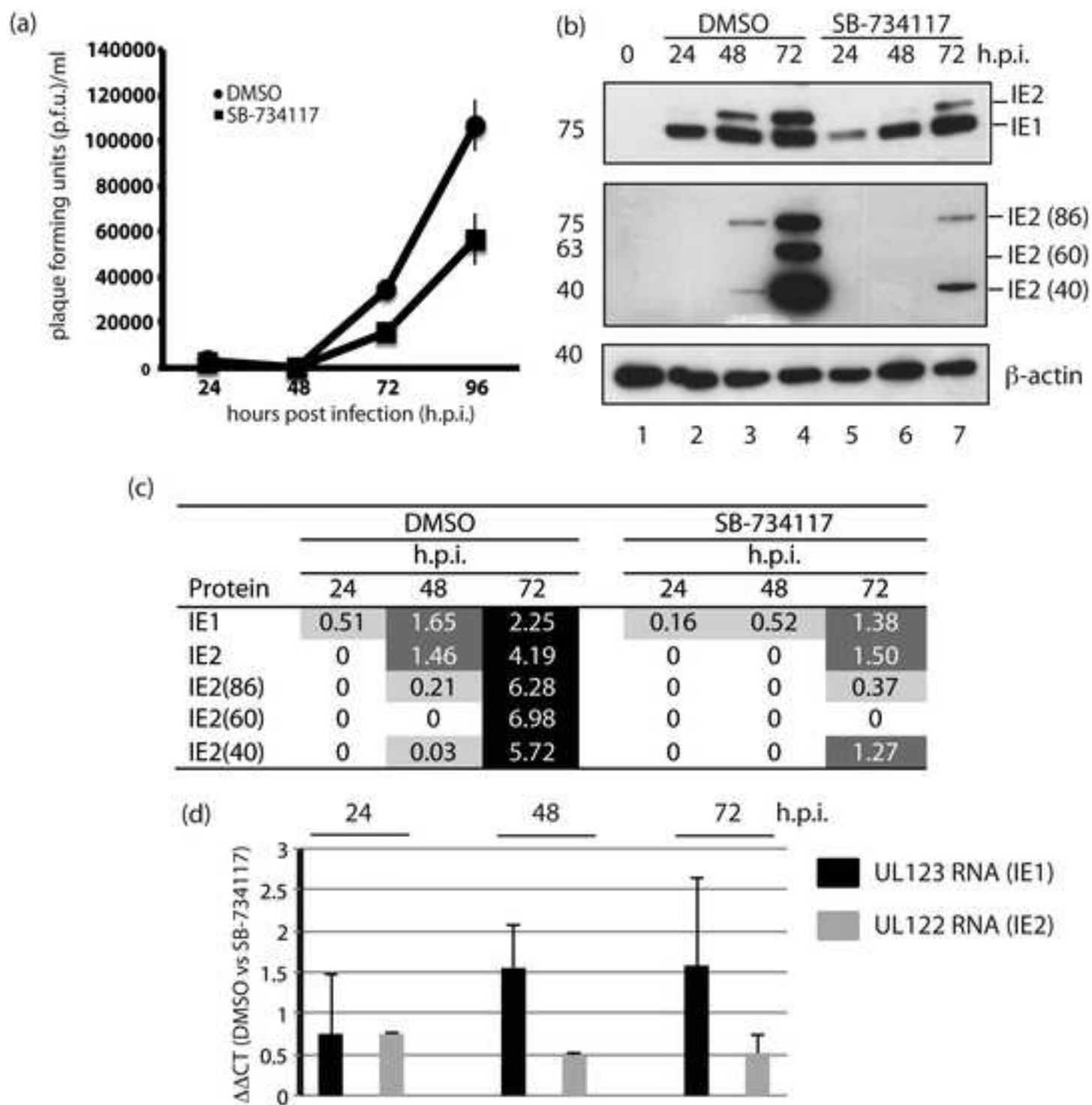
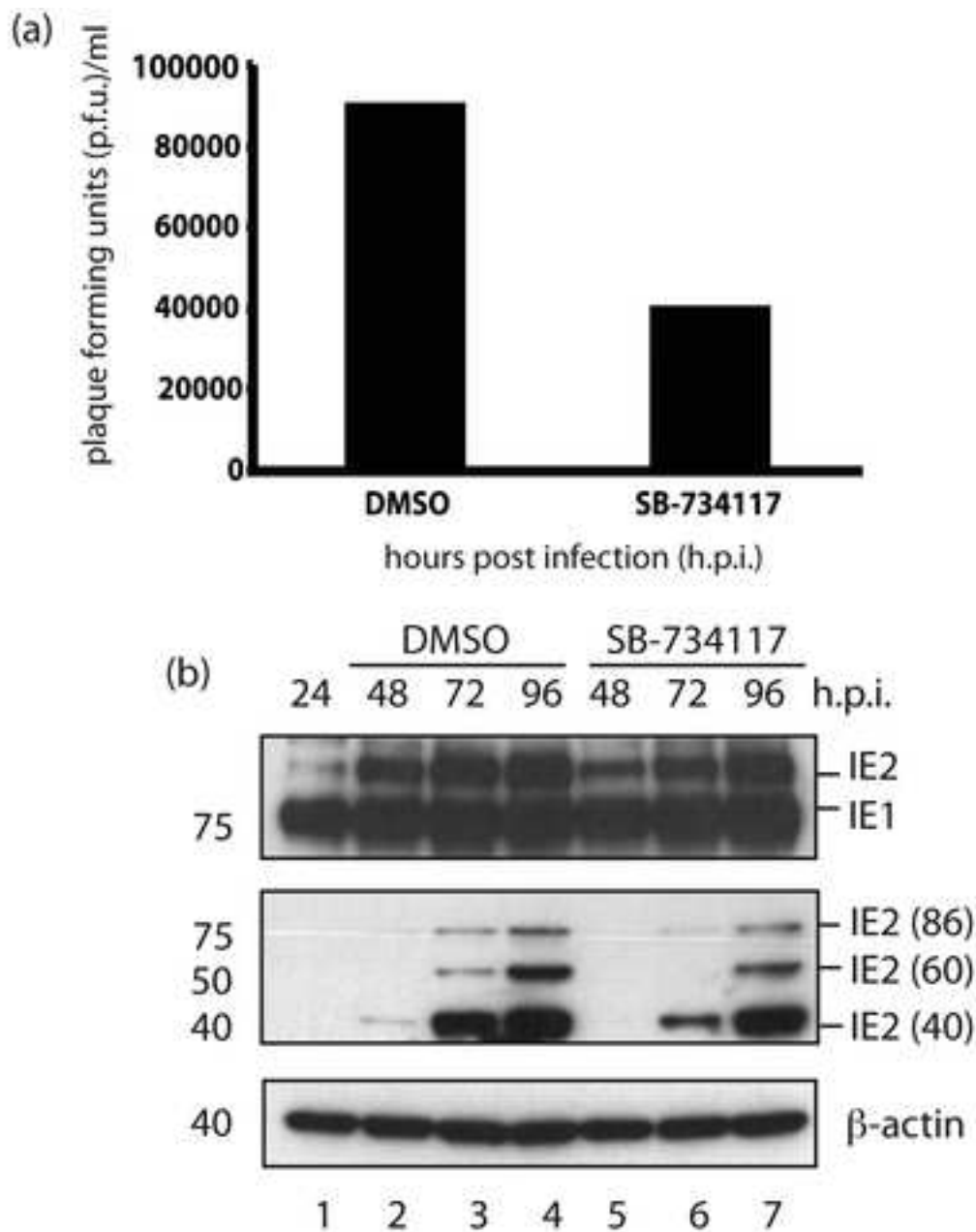


Fig. 3



(c)

Protein	h.p.i. 24	DMSO			SB-734117		
		h.p.i. 24	h.p.i. 48	h.p.i. 72	h.p.i. 24	h.p.i. 48	h.p.i. 72
IE1	1.10	1.10	1.00	1.02	1.02	0.81	0.87
IE2	0.11	0.81	1.32	1.08	0.62	1.32	1.74
IE2(86)	0	0	1.10	2.06	0	0.61	2.64
IE2(60)	0	0	0.23	3.66	0	0	2.92
IE2(40)	0	0.09	1.86	2.06	0	0.90	2.14

Fig. 4

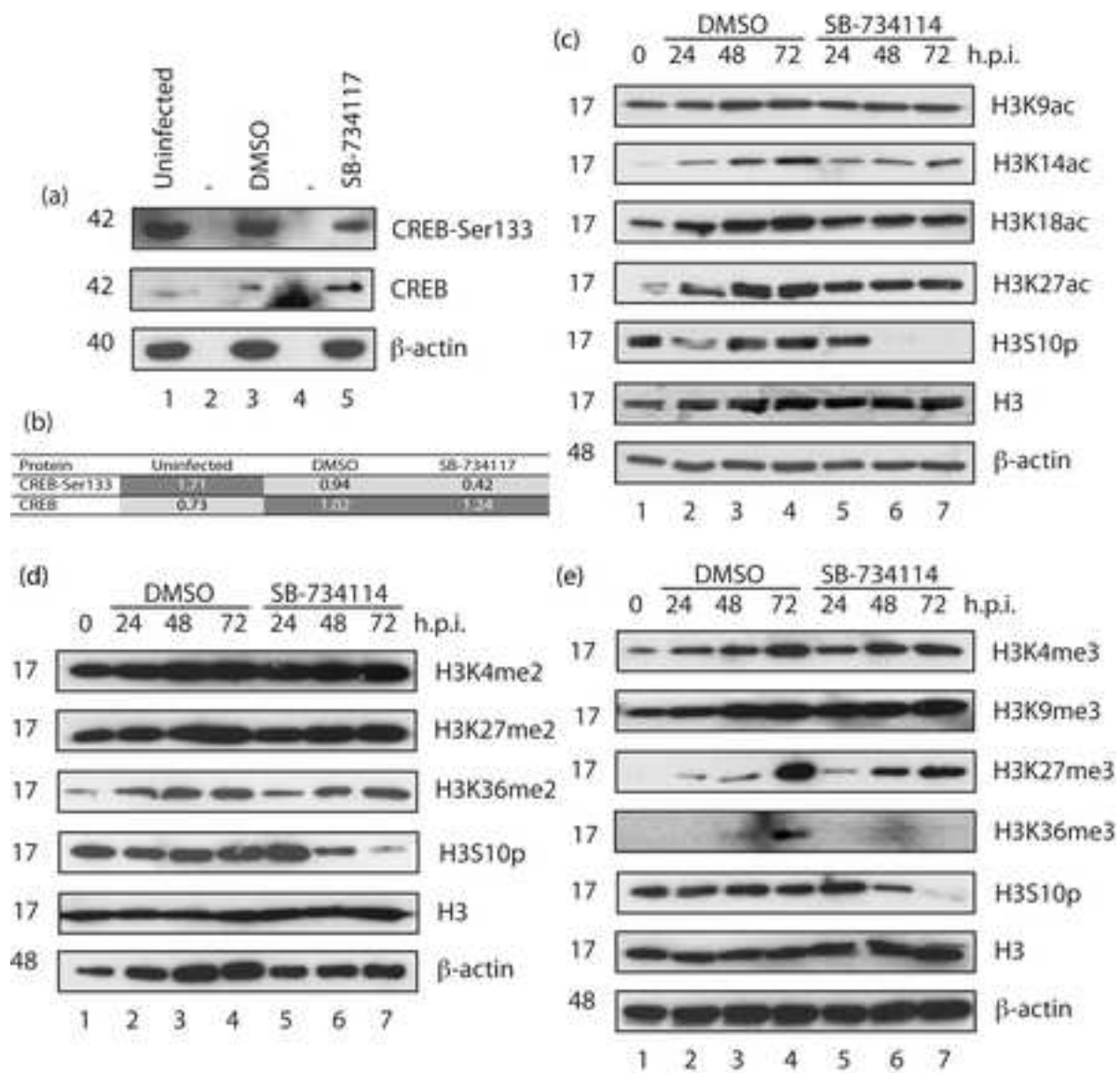


Fig. 5

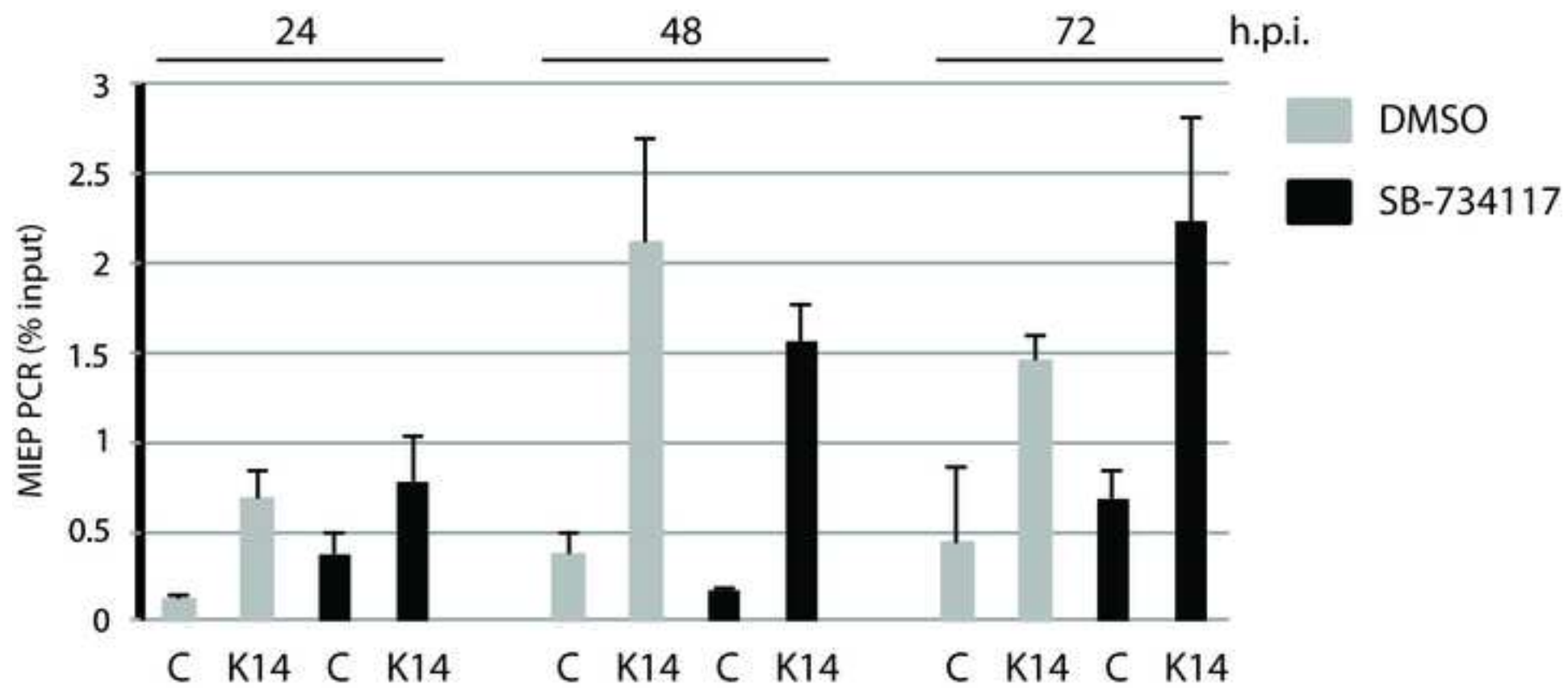


Fig. 6

SUPPLEMENTARY MATERIAL

High Throughput Screening of a GlaxoSmithKline Protein Kinase Inhibitor Set
Identifies an Inhibitor of Human Cytomegalovirus Replication that Prevents
CREB and Histone H3 Post-Translational Modification

Amina S Khan¹, Matthew J Murray², Catherine M K Ho¹, William J Zuercher³

Matthew B Reeves² & Blair L Strang^{1,4}

Institute of Infection & Immunity, St George's, University of London, London, UK¹;
Institute of Immunity & Transplantation, University College London, London, UK²;
Eshelman School of Pharmacy, University of North Carolina, Chapel Hill, NC,
USA³; Department of Biological Chemistry & Molecular Pharmacology, Harvard
Medical School, Boston, MA, USA⁴

Compound treatment and infection of cells for high throughput screening.

The GSK PKIS library [1] (stock concentration of 3.3 mM of each compound in DMSO) was screened in duplicate. Twenty four hours before infection 2000 HFF cells were seeded in each well of each Corning 384 plate. Unless stated otherwise, liquid was added to wells using a WellMate apparatus. At the time of infection, media was removed with a suction manifold and 30 µl of complete media was added to each well. Compounds were added to the plate containing HFF cells using a 100 nl pin transfer on a liquid handling robot. Negative and

positive controls (water+0.3% DMSO or heparin sulfate (5 $\mu\text{g/ml}$) + 0.3% DMSO, respectively) were added to plates by hand (12 wells of each). Cells were then infected with HCMV strain AD169 (MOI 1) in a total volume of 5 μl . Thus, the final concentration of compound in each well was 9.4 μM . Infected cells were incubated for 72 hours at 37°C, then prepared for analysis.

Preparation of screening plates for high throughput microscopy analysis.

Cell culture media was removed from infected cells and replaced with 20 μl Hoechst 33342 (SIGMA) diluted in PBS to a final concentration of 10 $\mu\text{g/ml}$. After incubation for 1 hour at 37°C, 20 μl of Deep Red Cell Mask (Invitrogen) (diluted in PBS to a concentration of 5 $\mu\text{g/ml}$) was added to each well. Cells were incubated for a further 5 min at 37°C. Cells were then fixed by removing PBS containing Hoechst and Cell Mask and adding 50 μl of 3.5% Formaldehyde (SIGMA) in PBS to each well. After incubating at room temperature for 10 min, fixative was removed and 50 μl of PBS containing 0.5% TritonX-100 was added per well to permeabilize cells. After 10 min incubation at room temperature, PBS containing detergent was removed, and cells were washed once with PBS. PBS was removed and replaced with 20 μl MAb P207 recognizing pp28 (Virusys) (dilution 1:1000) and anti-mouse secondary antibody conjugated to fluorophore Alexa488 (Molecular Probes) (dilution 1:1000). Plates were incubated at 37°C for 1 hour. After incubation, PBS containing antibodies was removed and replaced with 50 μl of PBS. Plates were then analyzed using automated microscopy for the presence of pp28 protein.

Microscopy analysis of screening plates. Infected cells stained with antibody to detect pp28 were imaged on an Image Express Micro (IXM) microscope (Molecular Devices) at 10x magnification to detect 3 wavelengths; 488 nm to detect antibody recognizing pp28, 568nm to detect Deep Red CellMask and 350 nm to detect Hoescht 33342 stain bound to nuclear DNA. Three images were captured from each wavelength in each well of the 384-well plate. The number of cells positive at all 3 wavelengths and percentage of pp28 positive cells in each well was determined using the Metamorph Multiwavelength Cell Scoring software (Molecular Devices). Typically, approximately 60% of cells were infected in wells treated with negative control, DMSO (data not shown).

Analysis of screening results. To assess the quality of data that could be returned from the screening protocol we calculated the Z'-factor [2, 3] derived from the positive (heparan sulphate treated infected cells) and negative (DMSO treated infected cells) control wells. The screening controls returned Z'-factors of greater than or equal to 0.5, indicating a robust separation of difference in the data derived from positive and negative controls (data not shown). Thus, the screening protocol could be reliably used to screen the compound collection.

After screening of the compound collection, data was discarded from any well in which the number of cells stained with Hoescht 33342 fell below 2-fold of the mean of the number of cells in each well of the plate. The data from the remaining wells from each plate was converted to a z-score (the number of

standard deviations from the mean of the data [2, 3]) and the average z-score from data in duplicate plates was determined. Images chosen at random were visually inspected throughout image capture and analysis to ensure raw data was consistent with z-scores.

Characterization of compounds within the GSK PKIS collection.

Characterization of compounds has been reported by Elkins and co-workers [4]. Kinase profiling was previously performed by using the Nanosyn microfluidics capillary electrophoresis technology (based on the change in electrophoretic mobility of a substrate upon phosphorylation) to determine each compounds ability to inhibit a panel of 224 recombinant kinase proteins. GPCR screening using calcium mobility assays was carried out as previously described [4]. The structure of each compound is available at ChEMBL (<https://www.ebi.ac.uk/chembl/>) [1].

Primary and secondary antibodies used in western blotting. Membranes were probed with antibodies recognizing IE1/2, UL44, pp28, UL84 (all Virusys, 1:1000 dilution), IE2 proteins (clone 5A8.2, Millipore, 1:1000 dilution), β -actin (SIGMA, 1:5000 dilution), CREB (product no. 06-863) or CREB-Ser133 (product no. 06-519) (both Millipore, 1:500 dilution). Antibody recognizing UL97 [5] was a kind gift from Donald Coen (Harvard Medical School, USA), respectively. All antibodies recognizing histone proteins were obtained from Cell Signaling Technology (products #9927, #9847, #9783) and used as per suppliers instructions. All primary antibodies were detected using anti-mouse- or anti-

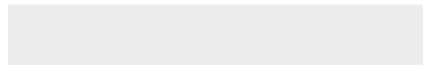
rabbit-horseradish peroxidase (HRP) conjugated antibodies (Millipore and Cell Signaling Technology, respectively). Chemiluminescence solution (GE Healthcare) was used in each case to detect secondary antibodies using film.

1. **Drewry DH, Willson TM, Zuercher WJ.** Seeding collaborations to advance kinase science with the GSK Published Kinase Inhibitor Set (PKIS). *Current topics in medicinal chemistry.* 2014;14:340-342.
2. **Birmingham A, Selfors LM, Forster T, Wrobel D, Kennedy CJ, et al.** Statistical methods for analysis of high-throughput RNA interference screens. *Nature methods.* 2009;6:569-575.
3. **Zhang JH, Chung TD, Oldenburg KR.** A Simple Statistical Parameter for Use in Evaluation and Validation of High Throughput Screening Assays. *Journal of biomolecular screening.* 1999;4:67-73.
4. **Elkins JM, Fedele V, Szklarz M, Abdul Azeez KR, Salah E, et al.** Comprehensive characterization of the Published Kinase Inhibitor Set. *Nat Biotechnol.* 2016;34:95-103.
5. **Kamil JP, Coen DM.** Human cytomegalovirus protein kinase UL97 forms a complex with the tegument phosphoprotein pp65. *J Virol.* 2007;81:10659-10668.



[Click here to access/download](#)

Additional Material for Reviewer
blsGSKSuppTables - FINAL.xlsx





Click here to access/download

Additional Material for Reviewer

blsGSKscreen -

FINAL+revision3(v1)+trackchanges.docx